Journal of Materials Chemistry C

PAPER

View Article Online
View Journal | View Issue

Cite this: J. Mater. Chem. C, 2014, 2, 3625

Alkyl substituted dithienothieno[2,3-*d*;2′,3′-*d*′]-benzo[1,2-*b*:4,5-*b*′]dithiophenes as solution-processable hexathiaheptacenes†

Lie Chen,[ab] Martin Baumgarten,[a] Xin Guo,[a] Mengmeng Li,[a] Tomasz Marszalek,[a] Fares D. Alsewailem,[c] Wojciech Pisula[a] and Klaus Müllen*[a]

Received 13th December 2013
Accepted 22nd February 2014

DOI: 10.1039/c3tc32478h

www.rsc.org/MaterialsC

Solution-processable hexathiaheptacene dithienothieno[2,3-*d*;2′,3′-*d*′]benzo[1,2-*b*:4,5-*b*′]dithiophenes (**DTTBDT a–d**) with various alkyl groups were synthesized by triflic acid induced ring closure. UV/Vis absorption, photoluminescence spectroscopy and cyclic voltammetry combined with density functional theory quantum-chemical calculations were performed to determine the photophysical and the electrochemical properties of **DTTBDT a–d**. In addition, the new hexathiaheptacenes show liquid crystalline properties dependent on their alkyl chain length. As observed from differential scanning calorimetry and polarized optical microscopy compared with **DTTBDT a** and **b**, **DTTBDT c** and **d** exhibit thermotropic liquid crystalline textures due to the rigid conjugated skeleton and the flexible long alkyl chains. For all four derivatives, the structural analysis indicates the formation of lamellar structures in which, surprisingly, the molecules are poorly packed. This molecular disorder is the main reason for the low performance of the p-type field-effect transistors.

Introduction

In recent years organic semiconductors have gained much attention for applications in electronics such as high-performance organic field-effect transistors (OFETs) and organic photovoltaic cells (OPVs).[1] The progress in the field of organic electronics is to a large part governed by the development of new, high-performance organic semiconductors. Generally, a high degree of intramolecular π-conjugation and close intermolecular stacking of organic semiconductor molecules are considered to be essential for their high-performance in field-effect transistors due to their high charge charier mobility. Pentacene has already demonstrated a charge carrier mobility of 1 to 5 $cm^2 V^{-1} s^{-1}$ in OFETs[2] (Scheme 1). However, pentacene suffers from poor stability due to a gradual destruction in the presence of oxygen, water vapor, and ozone.[3] An effective strategy to improve the stability of p-type organic semiconducting materials is the incorporation of fused thiophene rings into the acene structure, which can not only stabilize the HOMO level, but also preserve the close packing arrangement similar to that of pentacene, due to the strong intermolecular interactions between π⋯π and S⋯S, *etc.*[4] Although thiophenes are considered as electron rich, they indeed stabilize the HOMO level below −5 eV making the compounds air stable, while the corresponding heptaacenes with a higher HOMO tend to easy oxidation. Recently, the synthesis of fused linear acene bearing heteroatoms in their aromatic core has been described which showed improved stability toward photooxidation than their corresponding acenes,[5–8] and high charge carrier mobilities[7–10] have reached up to 10.0 $cm^2 V^{-1} s^{-1}$.[8]

In our previous study, we have developed a series of five-ring-fused pentacene analogues, with symmetrically fused thiophene-ring units (dithieno[2,3-*d*;2′,3′-*d*′]benzo[1,2-*b*;4,5-*b*′]-dithiophene, **DTBDT**, Scheme 1).[11] Solution-processed OFETs based on **DTBDT** with two linear hexyl chains revealed

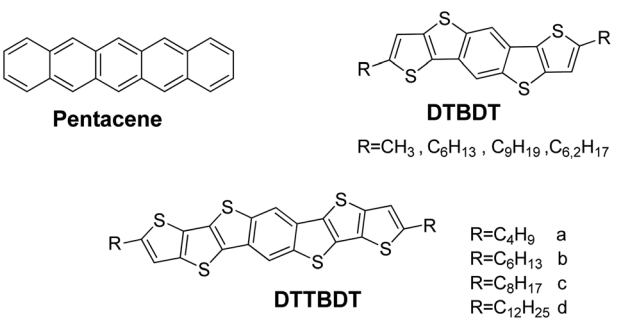

Scheme 1 Structures of pentacene, DTBDT and DTTBDT.

[a]Max Planck Institute for Polymer Research, Ackermannweg 10, D-55128 Mainz, Germany. E-mail: muellen@mpip-mainz.mpg.de; Fax: +49 6131 379100; Tel: +49 6131 379151

[b]Institute of Polymers, Nanchang University, 999 Xuefu Avenue, Nanchang 330031, China. E-mail: chenlienc@163.com

[c]Petrochemical Research Institute, King Abdulaziz Science and Technology, PO Box 6086, Ryadh 11442, Saudi Arabia

† Electronic supplementary information (ESI) available. See DOI: 10.1039/c3tc32478h

mobilities up to 1.7 $cm^2 V^{-1} s^{-1}$. This compound can also be solution processed into single monolayers or single-crystal microribbons that displayed values up to 3.2 $cm^2 V^{-1} s^{-1}$ due to their high order.[12,13] Furthermore, single-crystal microribbons of heteroheptacenes with extended planar frameworks, dithienothieno[2,3-*d*;2′,3′-*d*′]benzo[1,2-*b*:4,5-*b*′]dithiophene, displayed an OFET mobility up to 0.10 $cm^2 V^{-1} s^{-1}$, but the heteroheptacene was insoluble in common organic solvents.[14] The promising semiconducting properties of **DTBDT** inspired us to further explore the solution-processable heteroheptacene with the extended planar framework. In this work, we present a facile synthesis of a novel alkyl substituted dithienothieno[2,3-*d*;2′,3′-*d*′]benzo[1,2-*b*:4,5-*b*′]dithiophene (**DTTBDT**) (Scheme 1), with extended one-dimensional π-conjugation with respect to **DTBDT**. The coplanarity should promote the strong intermolecular interaction and enhance molecular packing in the solid states, which would be favorable for charge transport. Linear alkyl chains were attached onto the two molecular long-axis directions of the heteroheptacene skeleton in order to improve the solubility of the molecules for solution processability and to induce a distinct molecular packing. Interestingly, **DTTBDT** with longer alkyl chains form mesophases at elevated temperatures leading to liquid crystalline textures, while all compounds organize into disordered lamellar structures. Due to this poor order, the charge carrier mobilities are three orders of magnitude smaller than those observed for **DTBDT**.

Experimental section

Materials

Chemicals were obtained from Fluka, Aldrich, and Acros and used as received if not specified otherwise. The detailed synthesis of the alkyl substituted **DTTBDT** is presented in the ESI.†

Instruments

^1H NMR and ^{13}C NMR spectra were recorded in deuterated solvents such as CD_2Cl_2, THF using a Bruker DPX 250 spectrometer using the solvent proton or carbon signal as an internal standard. Field desorption (FD) mass spectra were obtained from a VG Instruments ZAB 2-SE-FPD. UV/Vis/NIR spectra were recorded at room temperature using a Perkin-Elmer Lambda 9 spectrophotometer. Fluorescence spectra were recorded using a SPEX-Fluorolog II (212) spectrometer. Cyclic voltammetric measurements were carried out in a conventional three-electrode cell using gold working electrodes of 2 mm in diameter, a platinum wire counter electrode, and a Ag/AgCl reference electrode using a computer-controlled PGSTAT12 at room temperature. MO calculations were carried out by the density functional theory (DFT) method at the B3LYP/6-31G(d) level using the Gaussian03 program package. XRD measurements were recorded using a Siemens D-500 powder diffractometer (Cu-Kα: 0.1541 nm) with a scan rate of 0.1°/20 s. 2D-WAXS measurements were performed using a custom setup consisting of the Siemens Kristalloflex X-ray source (copper anode X-ray tube, operated at 35 kV/20 mA), Osmic confocal MaxFlux optics, two collimating pinholes (1.0 and 0.5 mm – Owis, Germany) and an antiscattering pinhole (0.7 mm – Owis, Germany). The patterns were recorded using a MAR345 image plate detector (Marresearch, Germany). DSC was measured using a Mettler DSC 30 with a heating rate of 10 K min^{-1} from 20 °C to 300 °C. The optical textures of the hexathiaheptacenes were investigated using a Zeiss microscope with polarizing filters equipped with a Hitachi KP-D50 Colour digital CCD camera. The samples were sandwiched between two glass slides and then thermally treated using a Linkam hot stage regulated with a Linkam TMS 91 temperature controller. A Keithley 4200-SCS was utilized to measure the field-effect behaviour in a glovebox under nitrogen atmosphere.

Results and discussion

Synthesis of the alkyl substituted DTTBDT

Scheme 2 illustrates the synthetic procedure towards **DTTBDT a–d** with different linear alkyl chains and the synthetic details are provided in the ESI.† We reasoned that superacid-induced intramolecular cyclization reaction of aromatic methyl sulfoxides would be accessible to various fused thiophene derivatives.

With that in mind we studied two different synthetic approaches, route 1 and route 2, where the superacid-induced ring closure occurred from five-membered to five-membered ring in **6**, and from six-membered to five-membered ring in **10**, respectively. For route 1, **DTTBDT** was approached by intramolecular ring-closing condensation of the methylsulfinyl alkylthiophene with the adjacent thiophene in **6** (Scheme 2). Compound **4** is reported for the first time and was successfully prepared in four steps with good yields (ESI†). The Stille coupling of compound **4** and **5** was carried out in the presence of $[Pd(PPh_3)_4]$ catalyst with DMF as the solvent and afforded precursor **6** in a yield of 85%. Unfortunately, although the ring closure of the dimethylsulfinyl benzene with the adjacent thiophene proceeded well to prepare **DTBDT** induced by pure triflic acid, a similar approach to obtain **DTTBDT** by an intramolecular ring closure between methylsulfinyl thiophene and benzodithiophene units of **6** failed, even if performed with an excess of different acids, such as pure triflic acid and Eaton's reagent (7.7 wt% phosphorus pentoxide solution in methanesulfonic acid). The larger angle and stronger strain between the two thiophenes in **6** in comparison with the strain between the benzene and thiophene rings in **10** is probably responsible for this failure.

As consequence, an alternative synthetic route for the intramolecular ring closure of dimethylsulfinyl benzene with the adjacent alkylthieno[3,2-*b*]thiophene was designed (Scheme 2). 2-alkylthieno[3,2-*b*]thiophenes (**8a–d**) were synthesized starting from thieno[3,2-*b*]thiophene and 1-bromoalkane with *n*-butyllithium.[15] Lithiated 2-alkylthieno[3,2-*b*]thiophenes were reacted with Me_3SnCl to afford stannylated **8a–d** with high yield (>95%), which can be directly used in the next step without further purification. Compound **9** was easily obtained by following the procedure described in the literature.[11] Precursor **10** was made by Stille coupling of compound **8** and **9** with good yields (>80%). Subsequent ring closure of precursor **10** was

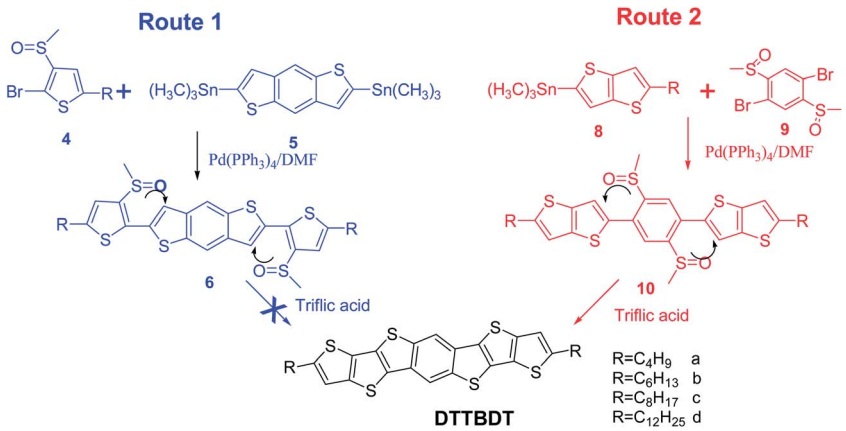

Scheme 2 Synthetic procedure for **DTTBDT a–d**.

carried out successfully in the dark for 3 days with an excess of triflic acid yielding **DTTBDT a–d** with four different linear alkyl chains $-C_4H_9$, $-C_6H_{13}$, $-C_8H_{17}$, and $-C_{12}H_{25}$, respectively. The green-blue solution was then poured into water to give a yellow green powder as the precipitate, followed by filtering, drying, and reflux in pyridine for demethylation. The products were purified by chromatography on silica, followed by two recrystallizations in hexane–THF. These heteroheptacenes can be dissolved in a common organic solvent, such as chloroform and THF. The compounds with octyl (**DTTBDT c**) and dodecyl (**DTTBDT d**) show higher solubility than those with shorter substituents, like butyl (**DTTBDT a**) and hexyl (**DTTBDT b**) groups. The structures of **DTTBDT** have been well confirmed from various methods (ESI†).

Optical properties

Fig. 1 shows the UV/Vis absorption spectra of **DTTBDT a–d** measured in dilute THF solution. All the samples exhibit identical absorption profiles in solution, where two absorption peaks at about 365 and 395 nm are ascribed to the π–π* transitions. Compared with the spectra recorded in solution, the absorption bands of their corresponding films are shifted about 15 nm to the longer region (Fig. S1†). The red shift absorption band is a typical signal of sulfur-rich linear thienoacene[16] and might imply a stronger intermolecular aggregation in the solid state compared with the solution that is desired for OFET applications. The optical energy gaps are about 3.06 eV for **DTTBDT a–d** determined by extrapolating the long-wavelength absorption edge in solution.

Upon photoexcitation at 380 nm, all heteroheptacenes exhibit blue fluorescence in THF solution, as shown in Fig. 2. With respect to **DTTBDT a–c** with relatively short alkyl chains, **DTTBDT d** with dodecyl substituents exhibits a red shifted emission maximum at ~450 nm, indicating an alkyl chain dependence emission of these compounds. In general, the film absorption spectra exhibit characteristic transitions that are bathochromically shifted relative to their solution values, which are indicative of the presence of π–π stacking in the solid state. For all solid state samples a broad and bathochromic emission well extending to 700 nm is observed, and the long alkyl chains favour a more distinct red-shift emission in **DTTBDT**. The alkyl chain dominates the optical properties in both solution and solid state.

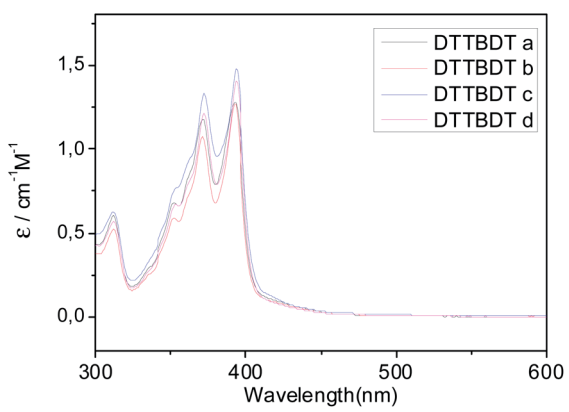

Fig. 1 UV/Vis absorption spectra of **DTTBDT a–d** measured in THF solution (1×10^{-6} M).

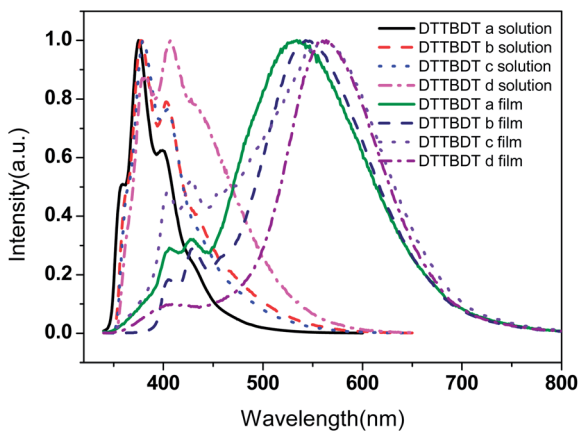

Fig. 2 Normalized photoluminescence (PL) spectra of **DTTBDT a–d** measured in THF solution and in films excited by irradiation of UV light of 380 nm.

Electrochemical properties

Cyclic voltammograms (CV) measurements were performed using a computer-controlled PGSTAT12 with a three-electrode cell in a solution of 0.1 M tetrabutylammonium hexafluorophosphate (Bu4NPF6) dissolved in THF at a scan rate of 50 mV s^{-1}. A Pt wire was used as the counter electrode and an Ag/AgCl electrode was used as the reference electrode. The voltammograms of **DTTBDT a–d** (Fig. S2†) exhibit similar and reversible oxidation waves, whereas within the accessible scanning range no reduction waves could be detected, implying a p-type semiconductor. The HOMO levels of −5.21 eV for **DTTBDT a–d** was estimated by the empirical equation $E_{HOMO} = -(E_{ox} + 4.4)$ eV and are obviously lower than that of pentacene (−5.14 eV).[17] The low-lying HOMO energy levels and relatively large energy gaps of 3.06 eV obtained from UV spectra promise an enhanced stability against oxygen under ambient conditions. However, the HOMO energy is about 0.35 eV higher and the HOMO–LUMO gap is about 0.30 eV lower than those for **DTBDT**,[11] due to the extended thiophene conjugated system. By taking into account their optical band gaps, which were derived from the absorption onset in the UV/Vis spectrum, the LUMO values are calculated to be ~2.15 eV.

To gain deeper insight into the electronic structures of the new heteroheptacenes, molecular-orbital (MO) calculations of the HOMO levels, LUMO levels, and band gaps were performed by using DFT methods (B3LYP, 6-31G*), which have been routinely used in the organic molecular calculation widely. For more convenient simulation, the alkyl group is replaced by the methyl group, where the electronic properties and equilibrium geometries will not be influenced significantly. It appears that the electron delocalized practically along the entire π-conjugated backbones well both on the HOMO and LUMO (Fig. 3). The HOMO of **DTTBDT** have an antibonding character (or intra-ring bonding) between the adjacent hetero rings and is delocalized over the molecular backbone, whereas the LUMO represents inter-ring bonding interactions, thus exhibiting a significant quinoid character. DFT-calculated HOMOs and LUMOs are qualitatively consistent with the results obtained from CV.

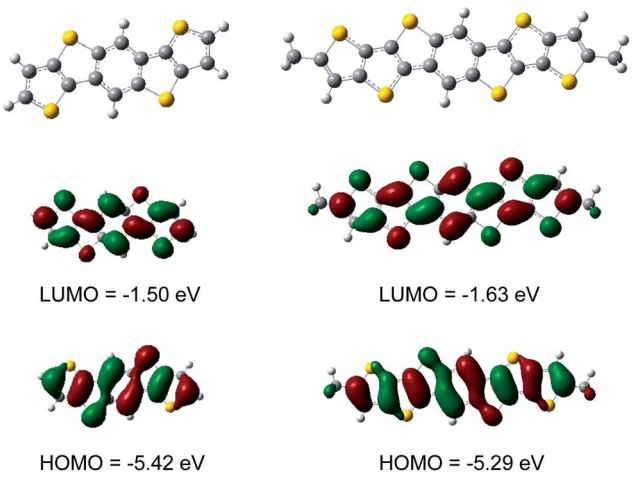

Fig. 3 DFT-calculated LUMOs and HOMOs of DTBDT (left) and DTTBDT (right).

Thermotropic properties

The thermal properties of the synthesized molecules were evaluated by means of thermogravimetric analysis (TGA) and differential scanning calorimetry (DSC) in a nitrogen atmosphere. TGA (Fig. S3†) reveals a 5% weight loss for all heteroheptacenes up to 360 °C suggesting the high thermal stability. From the DSC analysis two phase transition peaks were found during the heating and cooling process for **DTTBDT c** with octyl and **DTTBDT d** with dodecyl side chains indicating that the rigid conjugated skeleton and the flexible long alkyl chains induce a mesophase (Fig. 4a). **DTTBDT c** and **d** enter their mesostates during cooling from the isotropic melts at 240.9 °C (10.13 J g^{-1}) and 216.2 °C (5.03 J g^{-1}), respectively. This mesophase is stable in a temperature range over 65 °C for **DTTBDT c** and 93 °C for **DTTBDT d** before the compounds reach the low temperature state at 176.1 °C (2.92 J g^{-1}) and 123.8 °C (1.37 J g^{-1}). The small phase transition enthalpies suggest an identical nature of the low temperature state and mesophase. The results are confirmed by polarized optical microscopy (POM). After cooling **DTTBDT c** and **d** exhibit obvious optical anisotropy with birefringent textures suggesting thermotropic liquid crystallinity for both phases (Fig. 4c and d). Since **DTTBDT a** and **b** do not form a high temperature mesophase, these compounds do not show also such birefringent textures owing to their short alkyl chain. In general, the pronounced fluidity of liquid crystalline phases is promising for monodomain formation and self-healing of structural defects of organic semiconductors to improve the charge carrier transport over macroscopic dimensions.[18] However, an unhindered charge migration in mesophases also requires a tight packing of the building blocks. For this reason, in the next step the organization of the **DTTBDT** molecules was investigated.

The organization of **DTTBDT a–d** in thin films was studied using X-ray diffraction (Fig. 5). The films were prepared by drop-casting a 2 mg mL^{-1} chloroform solution. The thin films show only one Bragg peak of poor intensity corresponding to a *d*-spacing of 2.00 nm for **DTTBDT a**, 2.17 nm for **DTTBDT b**, 2.44 nm for **DTTBDT c** and 2.46 nm for **DTTBDT d** (Fig. 5a). This spacing is in agreement with the length of the long molecular

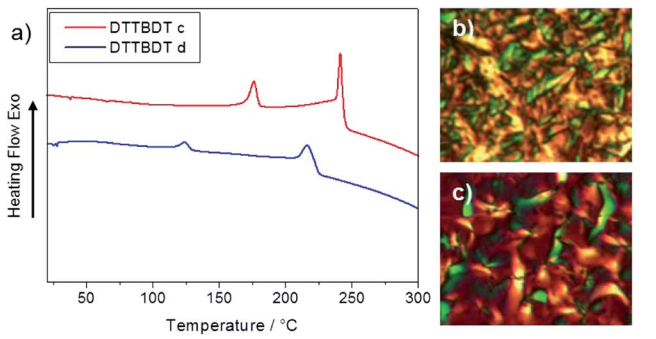

Fig. 4 (a) DSC thermogram of **DTTBDT c** and **d** recorded during cooling at a rate of 10 K min^{-1} and POM images of (b) **DTTBDT c** and (c) **DTTBDT d** displaying the birefringent textures after cooling at 1 K min^{-1}.

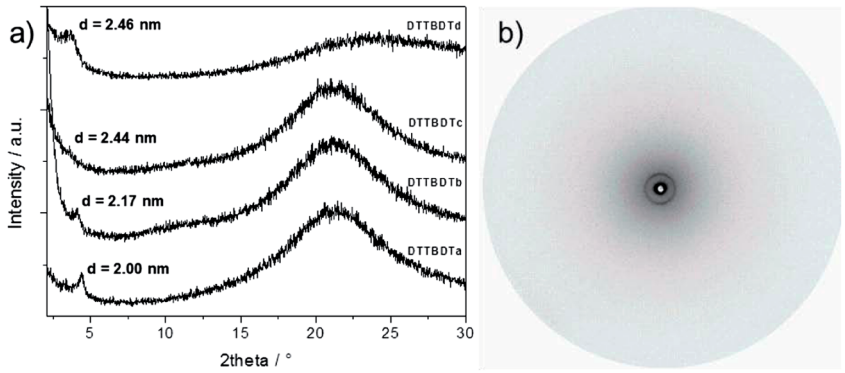

Fig. 5 (a) XRD of drop-cast films of **DTTBDT a–d** and (b) 2DWAXS of **DTTBDT c** powder.

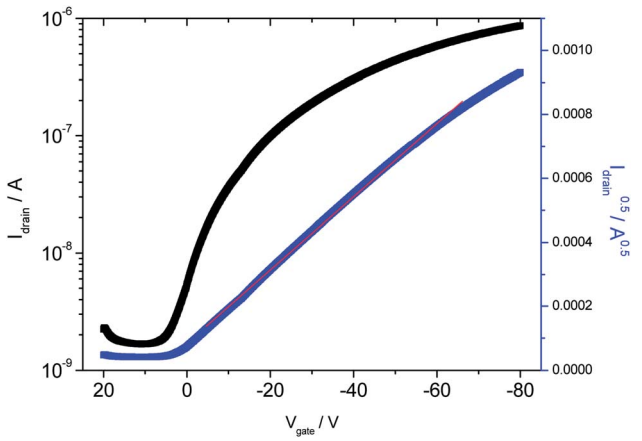

Fig. 6 FET transfer characteristics of **DTTBDT c** at a gate voltage of −80 V.

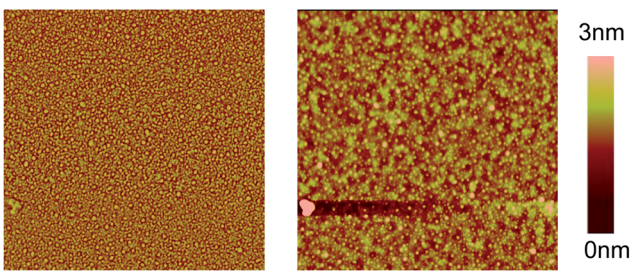

Fig. 7 Atomic force microscopy (AFM) phase (left) and height (right) images (3 μm × 3 μm) of the **DTTBDT c** film.

axis with the corresponding alkyl substituents and is related to a lamellar organization of the rod-like molecules. The lack of higher order peaks and the appearance of a pronounced amorphous halo are typical features for a short-range liquid crystalline ordering, while the absence of any scattering intensity in the wide-angle region suggests a disordered arrangement of the molecules within the lamellae. The poor order and the formation of a thermotropic LC phase even at ambient temperatures of 30 °C are quite surprising for a symmetric heteroacene of this large size carrying only linear alkyl side chains.[11,12] Typically, such kind of systems is highly crystalline leading to the formation of large crystals when deposited from solution.[11,12] Since the 1D XRD measurements provide information only about the out-of-plane organization in the film, a two-dimensional wide-angle X-ray scattering (2DWAXS) experiment for a powder sample of **DTTBDT c** was performed. The pattern in Fig. 5b exhibits just one small-angle isotropic reflection as already observed for the film without additional reflections in the wide-angle regions, which could be indicative for molecular packing. It can be assumed that the self-assembly of **DTTBDT** derivatives into the lamellar structure is mainly driven by a local phase separation between the rigid aromatic core and the flexible chains as the intermolecular π-stacking interactions seems to be weak.

OFET devices

To investigate the influence of the film ordering on the device performance, OFETs based on **DTTBDT** were prepared by drop casting a 2 mg mL^{-1} chloroform solution on silicon dioxide wafers. All FETs were fabricated employing the bottom-gate, bottom-contact architecture. Fig. 6 illustrates the transfer characteristics of **DTTBDT c**, and the performance of **DTTBDT a** and **d** is shown in Fig. S4.† All devices exhibit typical p-type transistor behaviour, while **DTTBDT c** reveals the highest hole mobility among the four oligomers of 2.6×10^{-4} cm^2 V^{-1} s^{-1} with on/off ratio of 10^3. Additionally, the poor performance of these compounds might be attributed to a discontinuous morphology consisting of a globular structure possibly hindering the charge transport by numerous grain boundaries, as evidenced by atomic force microscopy observations (Fig. 7). Again, this morphology significantly differs from the crystalline one observed for other heteroacenes and confirms the poor interaction between molecules.

In conclusion, we developed a successful strategy of synthesizing soluble hexathiaheptacenes with extended conjugation as p-type organic semiconductors. The rigid conjugated skeleton and the flexible alkyl chain induced a thermotropic behaviour for the **DTTBDT** oligomers. Surprisingly and atypically for heteroacenes, these compounds show low order and no packing leading to poor OFET performance. The exact reason for this behaviour is not fully understood since a pronounced

π-stacking interaction between the hexathiaheptacenes was expected. Apparently, the extension of the aromatic part does not lead to a tighter packing of the molecules. Based on these results, new design concepts towards high performance, small molecular organic semiconductors need to be developed.

Notes and references

1 (*a*) J. E. Anthony, *Chem. Rev.*, 2006, **106**, 5028; (*b*) K. Takimiya, S. Shinamura, I. Osaka and E. Miyazaki, *Adv. Mater.*, 2011, **23**, 4347; (*c*) C. Wang, H. Dong, W. Hu, Y. Liu and D. Zhu, *Chem. Rev.*, 2011, **112**, 2208.

2 (*a*) Y.-Y. Lin, D. J. Gundlach, S. F. Nelson and T. N. Jackson, *IEEE electron Device Lett.*, 1997, **18**, 606; (*b*) S. F. Nelson, Y.-Y. Lin, D. J. Gundlach and T. N. Jackson, *Appl. Phys. Lett.*, 1998, **72**, 1854; (*c*) T. W. Kelly, D. V. Muyres, P. F. Baude, T. P. Smith and T. D. Jones, *Mater. Res. Soc. Symp. Proc.*, 2003, **2**, 678; (*d*) D. H. Kim, D. Y. Lee, H. S. Lee, Y. H. Kim, J. I. Han and K. Cho, *Adv. Mater.*, 2007, **19**, 678.

3 (*a*) C. Pannemann, T. Diekmann and U. J. Hilleringmann, *Mater. Res.*, 2004, **19**, 1999; (*b*) A. Maliakal, K. Raghavachari, H. Katz, E. Chandross and T. Siegrist, *Chem. Mater.*, 2004, **16**, 4980.

4 (*a*) J. Huang, H. Luo, L. Wang, Y. Guo, W. Zhang, H. Chen, M. Zhu, Y. Liu and G. Yu, *Org. Lett.*, 2012, **14**, 133300; (*b*) Y. Zhou, W.-J. Liu, Y. Ma, H. Wang, L. Qi, Y. Cao, J. Wang and J. Pei, *J. Am. Chem. Soc.*, 2007, **129**, 12386.

5 H. Ebata, T. Izawa, E. Miyazaki, K. Takimiya, M. Ikeda, H. Kuwabara and T. Yui, *J. Am. Chem. Soc.*, 2007, **129**, 15732.

6 B. Tylleman, C. M. L. Vande Velde, J.-Y. Balandier, S. Stas, S. Sergeyev and Y. H. Geerts, *Org. Lett.*, 2011, **13**, 5208.

7 E. D. Głowacki, M. Irimia-Vladu, M. Kaltenbrunner, J. G. Siorowski, M. S. White, U. Monkowius, G. Romanazzi, G. P. Suranna, P. Mastrorilli, T. Sekitani, S. Bauer, T. Someya, L. Torsi and N. S. Sariciftci, *Adv. Mater.*, 2013, **25**, 1563.

8 A. N. Sokolov, S. Atahan-Evrenk, R. Mondal, H. B. Akkerman, R. S. Sánchez-Carrera, S. Granados-Focil, J. Schrier, S. C. B. Mannsfeld, A. P. Zoombelt, Z. Bao and A. Aspuru-Guzik, *Nat. Commun.*, 2011, **2**, 437.

9 P. Gao, D. Beckmann, H. N. Tsao, X. Feng, V. Enkelmann, W. Pisula and K. Müllen, *Chem. Commun.*, 2008, 1548.

10 T. Yamamoto and K. Takimiya, *J. Am. Chem. Soc.*, 2007, **129**, 2224.

11 P. Gao, D. Beckmann, H. N. Tsao, X. Feng, V. Enkelmann, M. Baumgarten, W. Pisula and K. Müllen, *Adv. Mater.*, 2009, **21**, 213.

12 S. Wang, P. Gao, I. Liebewirth, K. Kirchhoff, S. Pang, X. Feng, W. Pisula and K. Müllen, *Chem. Mater.*, 2011, **23**, 4960.

13 L. Li, P. Gao, K. C. Schuermann, S. Ostendorp, W. Wang, C. Du, Y. Lei, H. Fuchs, L. De Cola, K. Müllen and L. Chi, *J. Am. Chem. Soc.*, 2010, **132**, 8807.

14 Y. S. Yang, T. Yasuda and C. Adachi, *Bull. Chem. Soc. Jpn.*, 2012, **85**, 1186.

15 H.-S. Kim, Y.-H. Kim, T.-H. Kim, Y.-Y. No, S. Pyo, M. H. Yi, Y. D. Kim and S.-K. Kwon, *Chem. Mater.*, 2007, **19**(14), 3561.

16 Y. Liu, C. Di, C. Du, Y. Liu, K. Lu, W. Qiu and G. Yu, *Chem. – Eur. J.*, 2010, **16**, 2231.

17 M. L. Tang, T. Okamoto and Z. Bao, *J. Am. Chem. Soc.*, 2006, **128**, 16002.

18 W. Pisula, M. Zorn, J. Y. Chang, K. Müllen and R. Zentel, *Macromol. Rapid Commun.*, 2009, **30**, 1179.